SENSOR LETTERS
Vol. 6, 1–7, 2008

Self-Assembled Carbon Nanotube Multilayer Resistors and Nanotube/Nanoparticle Thin-Film Transistors as pH Sensors

Wei Xue and Tianhong Cui*

Department of Mechanical Engineering, University of Minnesota, Twin Cities, Minneapolis, MN 55455, USA

(Received: xx Xxxx xxxx. Revised/Accepted: xx Xxxx xxxx)

In this paper, we report the fabrication and characterization of two pH sensors using layer-by-layer self-assembled thin films. The first sensor uses a thin film as the sensing component which consists of alternating layers of single-walled carbon nanotubes (SWNTs) and polyelectrolytes. The second sensor is based on a thin-film transistor which has a nanotube/polyelectrolyte semiconducting film and a SiO_2 nanoparticle/polyelectrolyte dielectric film. The device fabrication process is inexpensive, solution-based, and can be done at room temperature. The sensors are highly sensitive to hydrogen ions in aqueous solutions with measured sensitivities of 9.7 and 179.8 μA/pH, respectively. The sensors respond linearly to pH solutions in the range of 5–9. This work introduces a new approach to fabricate inexpensive and high-performance pH sensors.

Keywords: Single-Walled Carbon Nanotube (SWNT), Layer-by-Layer (LbL) Self-Assembly, Thin-Film Transistor, pH Sensor.

RESEARCH ARTICLE

1. INTRODUCTION

Many types of microscale sensors have been developed for pH sensing applications including conductimetric sensors,[1] potentiometric membrane electrodes,[2] amperometric sensors,[3] luminescence systems,[4] and ion-sensitive field-effect transistors (ISFETs).[5] Among these devices, ISFET based biosensor is a promising method, which provides a number of advantages such as high sensitivity, fast response, and high robustness.[5–7] In addition, ISFET sensors require little pre-sampling, post-analysis, and routine maintenance in the laboratory.[8]

The basic design of the ISFET evolves from the traditional metal-oxide-semiconductor field-effect transistor (MOSFET) structure.[9] The two devices, ISFET and MOSFET, have similar structures and operate under the same principle. The main difference is instead of using a metal gate electrode directly attached to the surface, the ISFET uses a gate reference electrode inserted in an aqueous solution. The ion-sensitive property of ISFET broadens the application area of the traditional transistors. In addition, because ISFET sensors operate in aqueous solutions, they are considered to be the devices that bridge the gap between microelectronics and biotechnology. However, most reported ISFET pH sensors are silicon-based devices and the performance is restricted by the planar structures.[10] In contrast, nanomaterial-based electronic devices provide a powerful class of high-performance sensors. They have attracted significant fundamental research and commercial interests, and are highly desirable in interdisciplinary research fields. Among the nanomaterials, single-walled carbon nanotube (SWNT) has attracted considerable attention and been studied extensively. It is considered as one of the most promising candidates for sensing applications due to its inherent properties such as large surface area, high conductivity, and fast surface renewability.[11]

In this paper, we report two SWNT-based devices for pH sensing applications. The first sensor is based on alternating layers of SWNTs and poly(dimethyldiallylammonium chloride) (PDDA), a positively charged polyelectrolyte. The SWNT multilayer demonstrates an electrical conductivity change when exposed to pH solutions. The second device is based on the first sensor and also on our previously reported nanotube/nanoparticle thin-film transistors.[12] A SWNT/PDDA multilayer is used as the semiconducting film and a SiO_2 nanoparticle/PDDA multilayer is used as the dielectric film. The characterization

*Corresponding author; E-mail: tcui@me.umn.edu

 1546-198X/2008/6/001/007 doi:10.1166/sl.2008.m100

shows that both devices are highly sensitive towards hydrogen ion concentration in solutions. The structure, fabrication, and characterization of the two sensors are described and discussed in this report.

2. EXPERIMENTAL DETAILS

2.1. Materials

Pristine SWNTs (average diameter: 1.1 nm, average length: 50 μm, density: 2.1 g/cm^3) were purchased from Chengdu Organic Chemical Co., Ltd. The SWNTs were functionalized with a mixture of nitric and sulfuric acids (1:3 HNO_3:H_2SO_4) at 110 °C for 45 min.[13] This step introduced hydrophilic carboxylic groups (–COOH) on the nanotube sidewalls and open ends. After the acid funcationalization, the SWNTs were negatively charged and uniformly dispersed in deionized water with a concentration of approximately 1 mg/ml. SiO_2 nanoparticle dispersion (diameter 45 nm, Nissan Chemical Co.) was diluted with deionized water to a concentration of 40 mg/ml. Polyelectrolytes, including PDDA (molecular weight 200,000 to 350,000, polycation) and poly(sodium 4-styrenesulfonate) (PSS, molecular weight 70,000, polyanion) were obtained from Sigma-Aldrich. The concentrations of PDDA and PSS are 15 and 3 mg/ml, respectively. NaCl (0.5 M) was added to both polyelectrolyte solutions to increase the ionic strength.

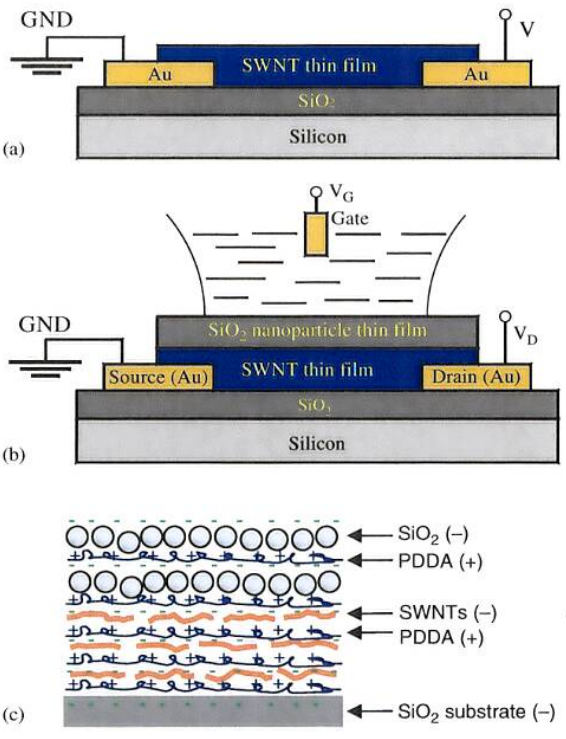

Fig. 1. The structure diagrams of (a) a thin-film resistor sensor, (b) a thin-film transistor sensor, and (c) self-assembled nanotube/nanoparticle multilayers.

2.2. Sensors Design

The structures of the sensors are illustrated in Figure 1. The sensors are fabricated on Si/SiO_2 substrates. The channel width and length of both devices are 5 μm and 1 mm, respectively. The first sensor is a thin-film resistor which includes two Au electrodes and a PDDA/SWNT multilayer film. The second sensor is based on a SWNT thin-film transistor. Au is used as the source/drain electrode material. An Ag/AgCl probe is used as the gate reference electrode in the aqueous solution. PDDA/SWNT and PDDA/SiO_2 nanoparticle multilayers are coated on the substrate as the semiconducting and dielectric films, respectively. The semiconducting channel conductivity is not only affected by the gate voltage, but also by the pH value of the solution. The hydrogen ions (H^+) in the solution introduce an additional input variable to the device and change its characteristics. Therefore, the drain current I_D is not only a function of the gate voltage, but also a function of the hydrogen ion concentration. Figure 1(c) shows the cross-sectional construction of the nanotube/nanoparticle multilayers of the thin-film transistor.

The thin-film resistor sensor has a similar structure to the transistor-based sensor. The only difference is that there is no PDDA/SiO_2 nanoparticle dielectric layer assembled on the surface. There is a high similarity between the two devices in many aspects including the fabrication processes, the device structures, and the corresponding measurement systems. Therefore, in the following sections, we use the transistor-based sensor to represent both devices unless there are major differences between them.

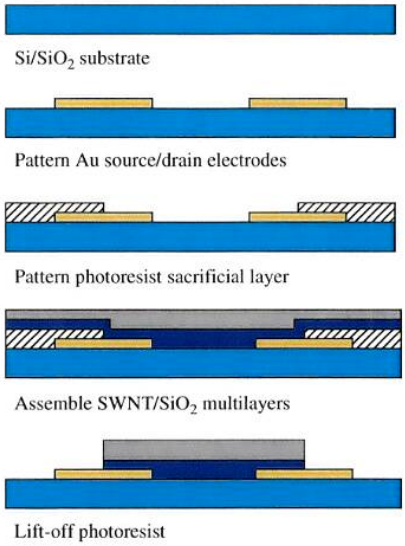

Fig. 2. Fabrication of the SWNT thin-film transistor sensor.

2.3. Fabrication

The fabrication process of the nanotube/nanoparticle thin-film transistor sensor is illustrated in Figure 2. The device is built on a standard 4-inch silicon wafer with a 300 nm thick SiO_2 layer on the surface. Metal layers of Cr/Au (100/200 nm) are deposited on the wafer by electron-beam evaporation process and then patterned as the source/drain electrodes. Next, another layer of photoresist is spin coated and patterned on the substrate as the sacrificial structure. The wafer is then alternatively immersed in PDDA and SWNT solutions for five times. Following the assembly of the $(PDDA/SWNT)_5$ semiconducting layer, SiO_2 nanoparticle multilayers are deposited on the substrate using the same layer-by-layer self-assembly technique. The assembly sequence for the PDDA/SiO_2 nanoparticle dielectric layer is $[PDDA\ (10\ min) + SiO_2\ (4\ min)]_6$. Both SWNT and SiO_2 nanoparticles are negatively charged and require the positively charged PDDA intermediate layers as the electrostatic "glue." Finally, the wafer is soaked in acetone for a lift-off process to expose the source/drain electrodes.[14]

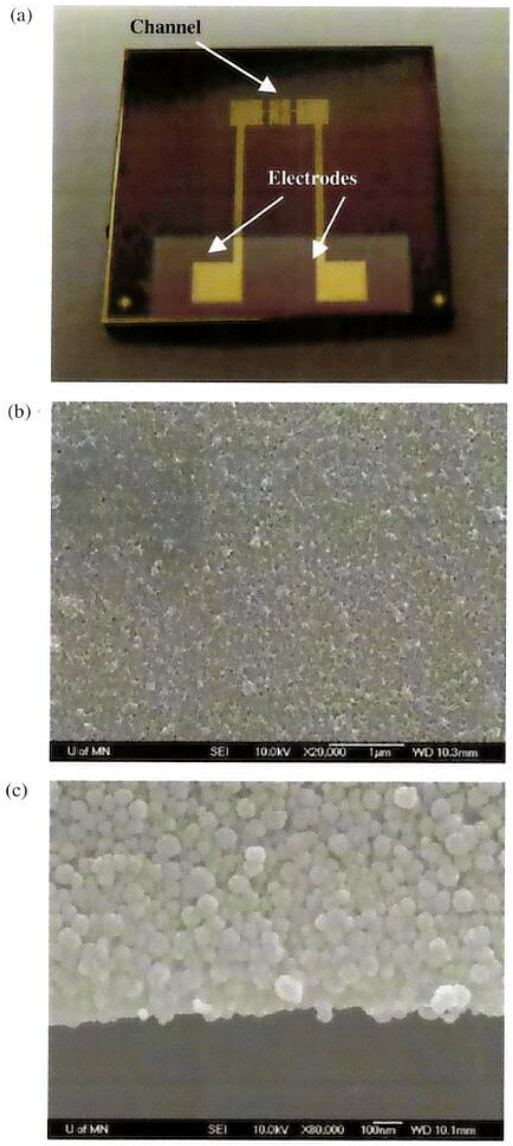

Fig. 3. (a) An optical image of a fabricated sensor. SEM images of the self-assembled (b) SWNTs and (c) SiO_2 nanoparticles.

The fabricated devices are inspected with an optical microscope and a scanning electron microscope (SEM). Figure 3(a) shows an optical image of a fabrication thin-film transistor sensor. The dimension of this device is 1×1 cm. The sensing channel, highlighted by an arrow, is much smaller, with width and length of 5 μm and 1 mm, respectively. The electrodes are elongated to the edge of the device for probing and detection. The SEM images of the self-assembled SWNTs (Fig. 3(b)) and SiO_2 nanoparticles (Fig. 3(c)) are also illustrated. The SWNTs and the particles are closely packed in the film.

3. RESULTS AND DISCUSSION

3.1. Thin-Film Resistor as pH Sensor

The SWNT thin-film resistor is characterized with a semiconductor parameter analyzer (HP 4156A). The device is partially immersed in pH solutions with the channel area totally submerged and the electrodes remain exposed in the air. One electrode is connected to the ground (GND) and a voltage of 0.75 V is applied to the other electrode, as shown in Figure 1(a). The current flowing through the channel, I, is recorded by the analyzer. The pH solutions are mixtures of 50 mM KH_2PO_4 and K_2HPO_4 buffers. The pH values range from 5 to 9. All the measurements are done in aqueous environment at room temperature.

The relationship between the measured current of the SWNT thin-film resistor and the pH value of different buffer solutions is illustrated in Figure 4. The solid triangles represent the experimental data and the line represents the fit curve. This device shows a linear response towards pH values. Because the pH value represents the concentration of hydrogen ions, the measured results indicate that the current difference is induced by these additional hydrogen ions in the solutions. Our previous study shows that SWNT is a p-type material with holes as the majority charge carriers.[12] The hydrogen ions can diffuse into the SWNT multilayer film and join the holes as charge carriers. This phenomenon increases the conductance of the SWNT film in the channel region. The sensitivity of the sensor can be calculated as 9.7 μA/pH by measuring the slope of the fit line.

3.2. Thin-Film Transistor

The SWNT thin-film transistor can also be used for pH sensing applications. Before using this device as a sensor,

RESEARCH ARTICLE

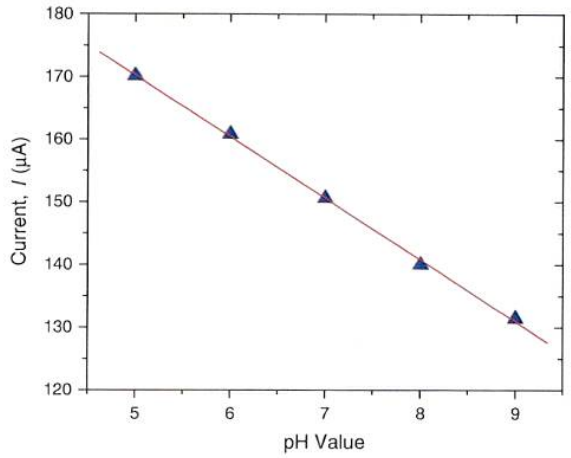

Fig. 4. The pH response of the SWNT thin-film resistor.

it is tested for its functionality—the field effect. Figure 5 shows the output and gate transfer characteristics of the transistor when it is immersed in a pH = 5 buffer solution. The Ag/AgCl gate reference electrode is also immersed in the pH solution and approximately 5 mm away from the channel. An explicit field effect can be observed from Figure 5(a): the drain current I_D is highly affected by the gate voltage V_G. In the characterization, the gate voltage V_G is swept from -2 to 0 V with a step of 0.4 V and the drain voltage V_D is swept from 0 to -1 V with a step of -20 mV. Both V_G and V_D are negative; i.e., the SWNT film shows p-type material characteristics in the aqueous environment. The gate transfer characteristics of the same device are obtained by fixing $V_D = -1$ V and sweeping V_G from 0 to -2 V with a -10 mV step, as shown in Figure 5(b). The left and right y-axes represent $(-I_D)^{1/2}$ and I_D, respectively. The threshold voltage $V_{th} = 1$ V is obtained by linearly extrapolating the $(-I_D)^{1/2}$–V_G curve to the x-axis. Only part of the curve, V_G from -1.25 to -2 V, is used for the extrapolation due to its relatively higher linearity than other parts. The hole mobility of the transistor is calculated as $\mu_p = 20.28$ cm^2/Vs using the traditional MOSFET equations. The on/off current ratio $I_{on/off}$ and the normalized transconductance are calculated as 2.55 and 0.31 S/m, respectively.

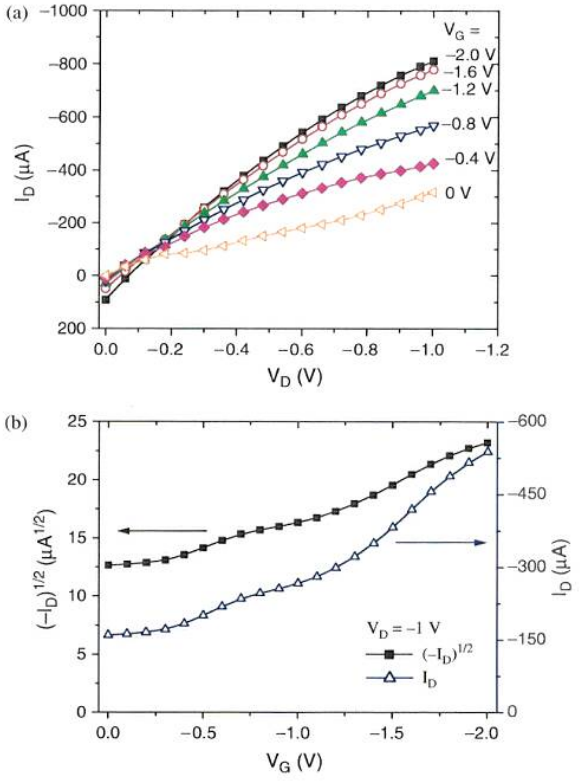

Fig. 5. (a) Drain current–voltage characteristics of an SWNT thin-film transistor in a pH = 5 buffer solution. (b) Gate characteristics of the same device at $V_D = -1$ V.

For a perfect field-effect transistor, the insulating layer has a high dielectric constant and can completely stop the diffusion of charge carriers from the conductive channel to the gate electrode. Therefore, the gate current $I_G = 0$. However, for the self-assembled thin-film transistor, a gate current can be observed and it is dependent on the gate voltage, as shown in Figure 6. The gate current can be considered as a leakage current which represents the motion of charge carriers inside the dielectric layer. A high leakage current $I_G = 92.5$ μA is observed at $V_G = -2$ V and $V_D = 0$ V. The leakage current is caused by the presence of the polyelectrolytes in the dielectric multilayer thin film. In air, the polyelectrolytes can be considered as insulators with high dielectric constants in the range of 30–120.[15] In the aqueous environment, however, they become conductive again. Therefore, some holes can drift from the semiconducting layer to the gate electrode through these

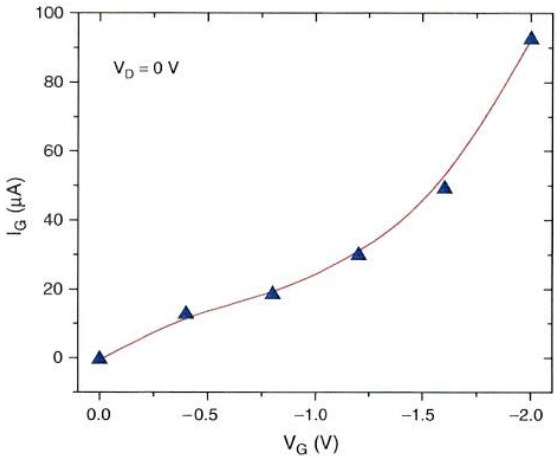

Fig. 6. Gate leakage current with respect to gate voltage. V_D is fixed at 0 V.

expanded polyelectrolytes. The motion of the charge carriers appears as the gate leakage current. One possible method to solve the problem is to use plasma-enhanced chemical vapor deposition (PECVD) to coat the dielectric layer. The PECVD technique can deposit a highly insulating SiO_2 film and reduce the leakage current. However, the PECVD process increases the fabrication cost of the devices.

3.3. Thin-Film Transistor as pH Sensor

The pH sensitivity of the SWNT thin-film transistor is measured by immersing the device in the pH solutions. The drain voltage V_D is swept from 0 to -1 V with a step of 10 mV and the gate voltage V_G is fixed at -2 V. The drain current I_D is highly dependent on the pH values, as shown in Figure 7. A lower pH value, or a higher H^+ concentration, induces a higher current. The recorded currents at different pH solutions are extracted and plotted as a pH-current curve in Figure 8.

Figure 8 compares the pH-current characteristics of the thin-film transistor with the same drain voltage $V_D = -1$ V and two different gate voltages $V_G = -2$ and 0 V. Both pH-current curves illustrate high linearity. The gate voltage has a high influence on the sensitivity of the transistor: when $V_G = -2$ V, the sensitivity of the device is calculated as 179.8 μA/pH; when V_G is decreased to 0 V, the sensitivity is measured as 11.88 μA/pH, which is approximately 15.1 times smaller. The drain current ranges are also different: -407.8 to -1127 μA for Figure 8(a) and -252.4 to -299.9 μA for Figure 8(b). Apparently, a higher gate voltage $|V_G|$ induces a higher drain current $|I_D|$.

The gate voltage V_G determines the magnitude of the drain current and controls the sensitivity of the device. It attracts holes in the SWNT semiconducting layer and causes the hole accumulation below the SWNT-SiO_2 interface. A higher $|V_G|$ is able to attract more holes and

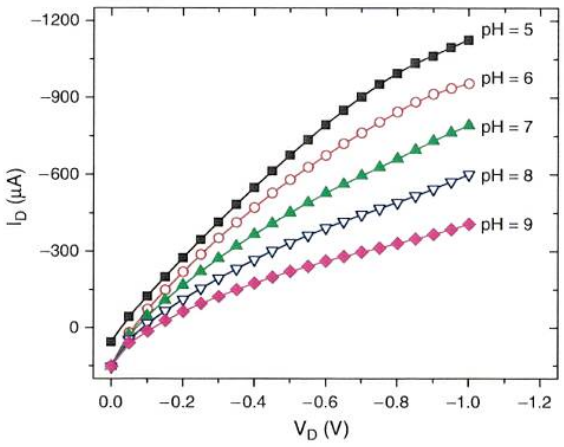

Fig. 7. Drain current of the SWNT thin-film transistor in different pH solutions. The gate voltage $V_G = -2$ V.

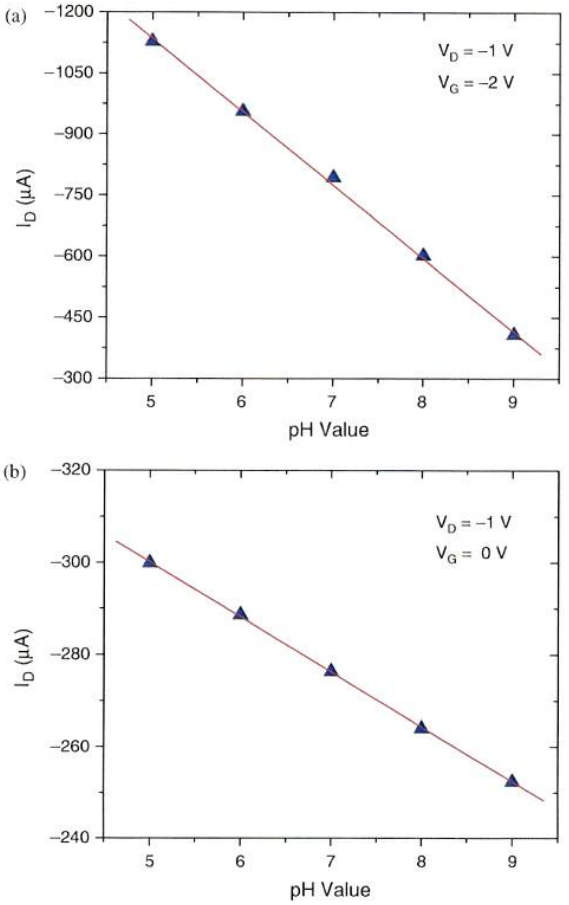

Fig. 8. Characterized pH sensitivity of the SWNT thin-film transistor with (a) $V_G = -2$ V and (b) $V_G = 0$ V. $V_D = -1$ V.

therefore induces a higher drain current $|I_D|$. The current change due to the pH variation is enhanced as well. Compared with the SWNT thin-film resistor, the transistor sensor shows a dramatically enhanced sensitivity with a factor of $179.8/9.7 = 18.5$.

To estimate the noise level, the sensor is submerged in deionized water with a data acquisition system connected for real-time measurement. The sensor operates under a quasi-idle condition: the gate voltage V_G is set as 0 V, and the drain voltage is set as -1 V to imitate the typical operational environment. A resistor with $R = 500$ Ω is added to the series circuit for device protection. The current is recorded and shown in Figure 9. The current of the sensor is measured as -167.4 $\mu A \pm 5\%$. The noise is mainly caused by the expanding and floating of the PDDA molecules and SWNTs due to their long-chain structures.

Although the SiO_2 nanoparticles and SWNTs are assembled on the device and held together by the PDDA electrostatic "glue," they may gradually diffuse away from the sensor surface. Therefore, it is important to study the long-term stability of the sensor. The SWNT thin-film transistor

RESEARCH ARTICLE

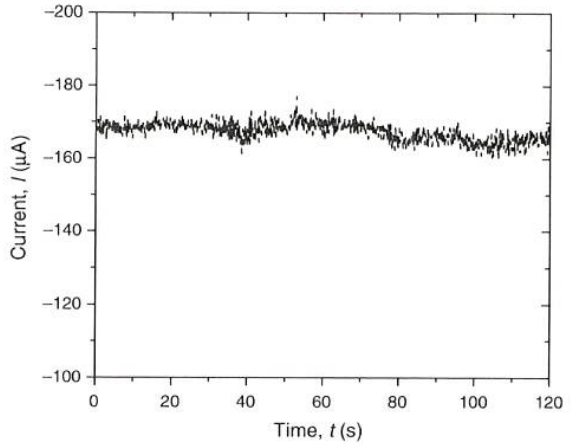

Fig. 9. Recorded current of the sensor at a quasi-idle condition. $V_G = 0$ V and $V_D = -1$ V.

is characterized in a pH = 6 buffer solution; the conditions are $V_G = -2$ V and $V_D = -1$ V for all the measurements. In this investigation, the sensor is first submerged in the solution and tested by the semiconductor parameter analyzer; then it is naturally dried and stored in air at room temperature for 24 hours; and it is tested again under the same condition. The procedure is repeated for 8 days. The stability of the sensor is illustrated in Figure 10. The average current is recorded as −974.1 μA and the standard deviation is approximately 54.8 μA. Compared with most silicon-based ISFET sensors, the stability of this device is relatively low. One reason is that the key components of the sensor are composite films. During the soaking and drying cycles, the assembled materials inside the films, especially the SWNTs, may slightly change their positions and directions. We suspect that the interconnection change between the SWNTs is the main reason for the long-term current variation of the sensor. A more densely assembled SWNT film may be able to minimize the variation and enhance the long-term stability of the sensor.

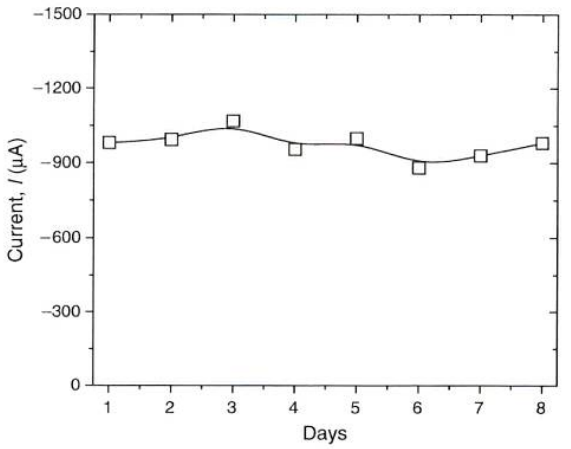

Fig. 10. Stability of the SWNT thin-film transistor in a pH = 6 solution. $V_G = -2$ V and $V_D = -1$ V.

Since the development of the first device in 1970,[9] ISFETs have made tremendous progress in the past 38 years. Several review papers have been published and the ISFET-technology has been summarized from different points of view.[7, 16] However, the traditional ISFET sensors are based on silicon which is beyond the scope of this paper. Some researchers have investigated the ISFET-technology using novel materials including nanomaterials. Luo et al. reported a MnO_2 nanoparticle-based pH sensor using a commercially available ISFET transducer.[17] The sensors demonstrate good performance with a pH sensitivity of 18.6 mV/pH. However, the pH range is limited to 6.2–8.2 and the linearity is relatively low. Recently, Liu et al. developed an ISFET pH sensor using In_2O_3 nanoparticles as the semiconducting material.[18] The device shows a clear field effect as a thin-film transistor. However, when operated as a pH sensor, the device has a nonlinear pH-current curve: the sensitivities in the pH ranges of 5–7 and 7–9 are 24 and 1.3 μA/pH, respectively. Compared with the In_2O_3-ISFET sensor, the SWNT-ISFET sensor demonstrates higher sensitivity and linearity in a wider pH range of 5–9. The primary cause for this difference is that SWNTs have a much higher conductivity than In_2O_3 nanoparticles: the mobility of the In_2O_3 thin-film transistor is 4.24×10^{-3} cm^2/Vs, which is 4 orders lower than that of the SWNT transistor.[12, 19] These nanomaterial-based ISFETs are promising devices and show high potential as sensors. However, they are still in the early stage of the development and there are many areas need further investigation. We believe that with more research groups and efforts involved, the performance of these sensors can be dramatically increased in the near future.

4. CONCLUSIONS

In conclusion, we have fabricated two pH sensors using the self-assembled SWNT thin films. The nanotubes are deposited on the substrate using the layer-by-layer self-assembly technique. The fabrication is low cost, solution-based, and can be done at room temperature. Both devices show high linearity towards pH values ranging from 5 to 9. The thin-film resistor uses a SWNT multilayer as the sensing film. The hydrogen ions can penetrate into the film and increase its conductance. The thin-film transistor uses SWNTs and SiO_2 nanoparticles as the semiconducting and insulating materials, respectively. The transistor shows an explicit field effect in aqueous solutions. The sensitivity is characterized as 179.8 μA/pH, which is 18.5 times higher than the first device. Due to the high performance and low cost, the SWNT thin-film transistor sensor provides a high-potential technique for various sensing applications.

Acknowledgment: We thank Professor Stephen A. Campbell at the Department of Electrical and Computer

RESEARCH ARTICLE

Engineering at the University of Minnesota for using his laboratory with the electrical characterization. We thank the staff members in the Nanofabrication Center and the Characterization Facility at the University of Minnesota for their help with the experimental work. This work is partially supported by the Defense Advanced Research Projects Agency (DARPA) MEMS/NEMS Fundamental Research Program through the Micro/Nano Fluidic Fundamentals Focus (MF3) Center.

References and Notes

1. N. F. Sheppard, M. J. Lesho, P. McNally, and A. S. Francomacaro, *Sens. Actuators B* 28, 95 **(1995)**.
2. B. Liu, Y.-H. Yang, Z.-Y. Wu, H. Wang, G.-L Shen, and R.-Q. Yu, *Sens. Actuators B* 104, 186 **(2005)**.
3. I. Vostiar, J. Tkac, E. Sturdik, and P. Gemeiner, *Bioelectrochemistry* 56, 113 **(2002)**.
4. H.-C. Tsai and R.-A. Doong, *Biosens. Bioelectron.* 20, 1796 **(2005)**.
5. Y. V. Plekhanova, A. N. Reshetilov, E. V. Yazynina, A. V. Zherdev, and B. B. Dzantiev, *Biosens. Bioelectron.* 19, 109 **(2003)**.
6. Y.-L. Chin, J.-C. Chou, T.-P. Sun, H.-K. Liao, W.-Y. Chung, and S.-K. Hsiung, *Sens. Actuators B* 75, 36 **(2001)**.
7. P. Bergveld, *Sens. Actuators B* 88, 1 **(2003)**.
8. Y. Miao, J. Guan, and J. Chen, *Biotechnol. Adv.* 21, 527 **(2003)**.
9. P. Bergveld, *IEEE Trans. Biomed. Eng.* 17, 70 **(1970)**.
10. F. Patolsky and C. M. Lieber, *Mater. Today* 8, 20 **(2005)**.
11. J. Wang and M. Musameh, *Anal. Chem.* 75, 2075 **(2003)**.
12. W. Xue, Y. Liu, and T. Cui, *Appl. Phys. Lett.* 89, 163512 **(2006)**.
13. W. Xue and T. Cui, *Nanotechnology* 18, 145709 **(2007)**.
14. W. Xue and T. Cui, *Sens. Actuators A* 136, 510 **(2007)**.
15. C. Tedeschi, H. Möhwald, and S. Kirstein, *J. Am. Chem. Soc.* 123, 954 **(2001)**.
16. S. Martinoia, G. Massobrio, and L. Lorenzelli, *Sens. Actuators B* 105, 14 **(2005)**.
17. X.-L. Luo, J.-J. Xu, W. Zhao, and H.-Y. Chen, *Biosens. Bioelectron.* 19, 1295 **(2004)**.
18. Y. Liu and T. Cui, *Sens. Actuators B* 123, 148 **(2007)**.
19. T. Cui, Y. Liu, and M. Zhu, *Appl. Phys. Lett.* 87, 183105 **(2005)**.

RESEARCH ARTICLE